Computational Applications in Physical Anthropology

Midori Hyndman
Department of Computer Science
University of Toronto
mhyndman@cs.toronto.edu
http://www.cs.toronto.edu/ mhyndman

1 Introduction

2 Data Acquisition

The design and applicability of computational approaches for analysis of anthropological artifacts is dependent on the quality of the data regarding the specimen. The technology is available to retrieve high quality three-dimensional models of excavated objects, however, widespread use is often limited by cost or portability of the specimen and data acquisition tools. In this section the common data acquisition techniques are presented. A basic explanation of the methodology is provided along with its advantages and limitations.

2.1 Plain Film Radiograph

Radiography was first applied to archeological studies within a year of its discovery over two centuries ago (11). To create a plain film radiograph (also called a Roentgenograph) the fossil is placed between an x-ray source and x-ray sensitive film. Radiation passes through less dense areas while it is absorbed and scattered by the more dense material. As a result, all structures in the path of the x-ray beam are superimposed in the image.

Given the low contrast resolution and the superimposition many details are difficult to distinguish, however, the high spatial resolution of the image was advantageous for analysis. The ease of use, portability and affordability made this technique common for specimen documentation and analysis, in particular in comparative anatomy of primate cranial form (30) as shown in Figure 1*a*.

Widespread use of conventional radiography is also found in paleoradiological studies of mummies (11). Simple x-ray techniques allow for a virtual undressing of the mummy without cubersome transportation of the specimen, therefore, plain film radiography is encouraged for preliminary analysis (11). An application of plain film radiograph to mummified human remains is illustrated in Figure 2.

Plain film radiography has two significant disadvantages. First, there is a lack of detail due to the superimposition. Second, variable distortion is exhibited in the images since x-rays emerge from collimators as a diverging conical beam. Although this can be corrected to some degree with the appropriate set-up and the use of ~~transmitors~~ with parallel beams, it is more common to use an alternative imaging technique -computed tomography in particular. When applied to palaeontology, conventional radiographs have

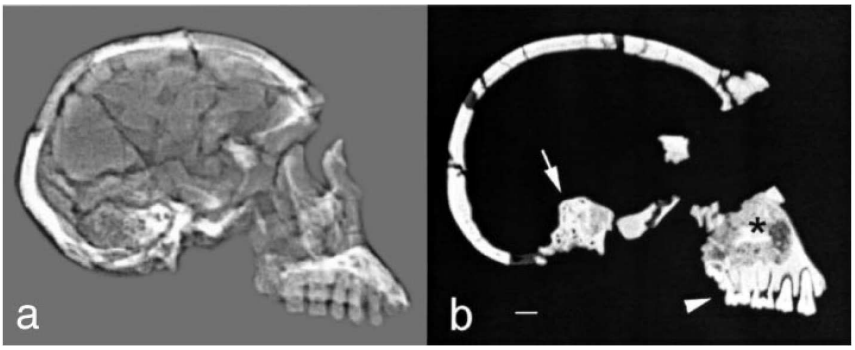

Figure 1: Imaging of *Homo ergaster* cranium from Spoor et al. (30) (*a*) Lateral plain film radiograph. (*b*) Parasagittal CT scan. The superposition of structures is the radiograph restricts the ability to distinguish details such as the root canals of the molars (indicated with the arrowhead) and the structures of the bony labyrinth (indicated with the arrow). Unlike radiography, CT scans can distinguish between fossil morphology and higher density sedimentary matter. Although not particularily clear to the non-specialist reader, this is apparently noticeable in the maxillary sinus (indicated with the asterix). Bar, 10 mm.

a further limitation: archeological specimens often coated with sedimentary material which is of higher density than the fossil itself blocking morphological information.

Inherent to the superimposition effect plain film radiography allows many structures to be compared in a single image. Spoor et al. (30) reasons that this planar projection of specimens has resulted in the portrayal of evolutionary changes as a two-dimensional rather than a three-dimensional process. Despite the availability and use of three-dimensional data acquision tools, two-dimensional analysis remains the norm.

2.2 Computed Tomography

Developed in the early 1970s, computed tomography was quickly embraced by acheologists. In computed tomography (CT), an x-ray source and a array of detectors rotate around the specimen obtaining 2-dimensional densitiy information for a slice shaped volume. For each slice, a fan beam of x-rays are transmitted through the object and the level of attentuation observed by the detectors provides absorption information which indicates material density. Multiple slices are captured as the x-ray source and detector are shifted along the length of the object, and combined these slices provide 3-dimensional density information about the scanned object. A simplified diagram of the process is shown in Figure 3. Example CT images are shown in Figures 1 and 2.

CT scanning avoids the problems associated with superimposition and measuring the attenuation in multiple directions removes parallax distortion artifacts. Although the spatial resolution is lower in cross-sectional CT images than in plain film radiographs, the contrast resolution is superior. In palaeontological applications the increase in contrast is especially useful for capturing the small density differences which distinguish sediment from bone. However, highly-mineralized or sediment filled fossils imaged with regular medical CT scanners often produce results with large amounts of noise or streaking artifacts. These artifacts are due to the overall density or mass exceeding the normal range

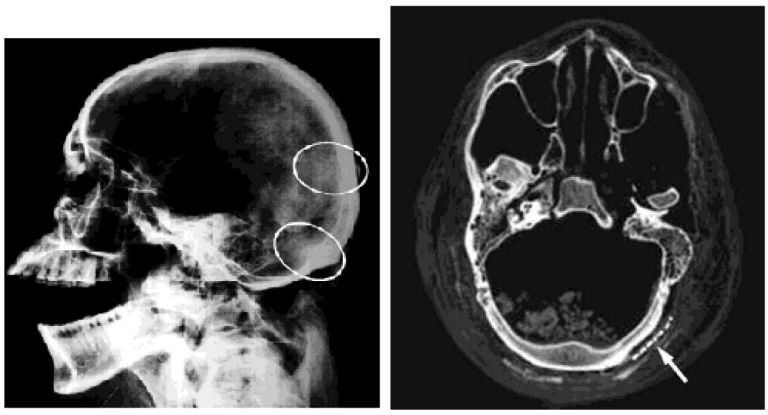

Figure 2: The lateral plain film radiograph of the Sulman Mummy skull shown on the left. The ovals highlight density differences which provided the first indication of foreign objects on the mummy. This image illustrates the advantageous high spatial frequency of conventional radiographic images. In the axial CT slice of the Sulman Mummy skull, shown on the right, the confirmation of beads is indicated by the arrow. Both images from Garner et al. (11).

found in patients.

The spatial resolution of a CT image depends on the geometry of the x-ray beam, although it is more often limited by a combination of the field of view and the number of pixels in the image. Medical CT scanners acheive a spatial resolution of approximately 0.3-0.5mm along the planar surface of the image and 0.5-1.5mm perpendicularly due to the thickness of the cross-sectional volumes. Micro-CT scanners provide a much higher resolution, typically obtaining square voxels between 1-200μm depending on the size of the specimen.(30)

Micro-CT scanners often operate differently ~~that~~ standard medical CT devices. Typically micro-CT scanners operate in the order of minutes per slice, rather than seconds. In many devices the specimen is rotated instead of rotating the source and array of dectors. ~~Also, not~~ all micro-CT scanners use a line of detectors to measure the x-ray attenuation. Some scanners use an image intensifier which intercepts the x-ray photons, converts them into visible light photons, and amplifies the light signal (35). The radiographic images from multiple directions are recorded using a framegrabber to obtain a 3D volume. Due to a limited dynamic range, image intensifiers cannot capture small differences in contrast therefore they are no longer useful for paleoanthropological applications which require the contrast difference to isolate sediment from mineralized bone (30).

Micro-CT scanners are not necessarily required for an analysis of bone density (22). Localized patterns of high apparent density are not altered significantly when using regular CT scanner instead of micro-CT scanner, despite the advantage of increased spatial resolution (2). For this reason, and due to the ~~substancially~~ higher cost, micro-CT technology is not widely used in the recent literature.

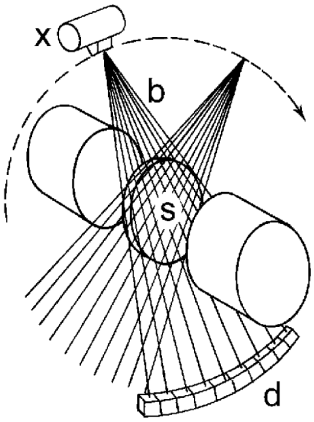

Figure 3: Diagram from Spoor et al. (30) illustrating the ~~principals~~ of CT scanning. The source (x) emits a fan beam of x-rays (b) and the array of detectors (d) rotate about the specimen and measure its attenuation within ~~the~~ a cross-sectional volume (s).

2.3 Magnetic Resonance Imaging

To obtain ~~an~~ Magnetic Resonance Image (MRI), the object is placed in a strong static magnetic field which aligns protons. A sequence of radiofrequency pulses are sent to flip the protons into a higher energy state and when the pulses cease, the protons return from the higher energy state to their original unexcited state emitting the difference in energy. This energy, or magnetic resonance signal, is read by a coil and mapped onto a 2D plane (or occasionally a 3D block). The intensity of the signal reflects the local proton concentrations and their chemical environment. In the context of human imaging, different tissues exhibit different concentration of fat and water, which emit MR signals of different intensities. Relative to soft tissues, mineralized bone emits a signal of very low intensity therefore appearing as a void in the image.

MRI technology and its applications are complementary to those of palaeoanthropological research in several ways. Research into the comparative and functional relationship between soft tissues and bone morphology within current populations provides data which can be mapped onto ancient specimens and used to model potential biomechanical properties (19). Also, patterns in ontogenetic development, largely studied with high-resolution MRI[1], could potentially provide valuable insight into the mechanisms of phylogenetic change (10).

2.4 Laser Scanning

Laser scanning has been used for decades to extract three-dimensional surface models of objects. The devices are often portable and more accessible than medical-CT scanners. Unfortunately the surfaces extracted are generally extremely noisy. The results rarely

[1] High-resolution MRI (hMRI) scans provide spatial resolution of approximately 156-300μm in-plane and 300-600μm in slice thickness. Clinical MRI units provide in-plane spatial resolution of 0.7-1mm with a slice thickness of 1-3mm. The higher-resolution requires the use of stronger magnetic fields and significantly longer imaging times -as much as 24 hours for a specimen.

reveal a closed manifold and often exhibit holes or surfaces intersect. Also, typically only one side of the object is captured. Despite these shortcomings laser scanning remains prevalent in the literature, used ~~as recently as~~ (38).

2.5 Contact devices

Three-dimensional coordinates can also be measured using contact digitizers, such as a pointing stylus which electromagneticallly provides relative location and orientation with 0.5mm accuracy (20). Coordinates are measured either from the original specimen or a stereolithographic replica of the virtual reconstruction.

Although common in the literature (12; 16; 20), contact devices have several limitations. Obtaining landmarks in this way is extremely tedious (38). Many ~~specimen~~ recovered over the last century, which are still under analysis, have undergone multiple reconstructions resulting in surface damage which adds noise. Moreover, some of these ~~specimen~~ remain in inaccurate physical reconstructions which prohibit access for certain measurements (an example is shown Figure 5). Furthermore, analysis of interior regions such as the sinuses and the molar cavities, cannot be accessed with surface-based devices (33; 41).

3 Post-processing

3.1 Merging Computed Tomography Data

Computed tomography scans consist of multiple two-dimensional slices of a matrix of density values. For paleontological applications, image filtering is used to isolate the fossil from the surrounding sediment in the matrix in each two-dimensional slice. Simple thresholding is often used to isolate the ~~bone, however this can~~ artifacts around edges of the specimen ~~due to~~ because spongious bone around the surface has a lower density (36). Interactive data segmentation tools are generally used for isolating the fossil fragments from the background (41). Techniques for isolating artifacts from CT scanned data is an area of research unto itself and is not described thoroughly in this review.

3.2 Thin Plate Splines

When contact digitizers are used to extract landmark positions on fossils, thin plate splines are commonly used to create surface models with the landmarks as control points. The accuracy of the resulting three-dimensional ~~model, depends~~ on the number of landmarks used in the approximation.

Thin plate splines are also commonly used to handle missing data in virtual models(5; 23; 41). For statistical ~~analysis~~ of multiple ~~specimen,~~ techniques such as principal component analysis require an equal number of landmarks. However, some fossils are incomplete. Estimating location of landmark dropouts by substituting the mean of all other specimen is unbiased, but underestimates standard error. Using thin plate splines and fitting the missing position to minimize the ~~different~~ in bending energy between the specimen and the reference image is statistical more robust. For example, Ponce De León et al. (23) estimate the endocranial volume by applying a three-dimensional thin-plate spline morphing to approximate missing fragments. Two separate ~~approximation~~ were

obtained by morphing a modern human skull and a well-preserved Neanderthal specimen. By fitting available corresponding landmarks on the specimen skull, the missing landmarks were assumed to correspond to those of the morphed skulls.

4 Reconstruction from fragments

Excavated historical artifacts are rarely found in their original state. Archeological finds are commons below the surface of the ground and therefore subject to pressure from the overlying strata. Context largely influences the effect of sedimentary deposits on the post-burial modification of skeletal remains and cultural artifacts. Alterations of the original chemical and structural properties of a specimen are governed by ~~diagenesis -the elemental~~ and mineralogical composition of bone, the enveloping soil, and the groundwater, climate and geological conditions in the local burial environment (39). Depending on the context, a specimen might undergo plastic deformation, fracture into scattered fragments, or both.

Reconstruction of excavated artifacts involves not only reestablishing the spatial relationship of scattered fragments based on anatomical indicators, but also correcting the sequence of post-burial alterations and deformations in reverse temporal order (24). The ~~recontruction~~ process aims to determine the in vivo state or original form of the specimen.

There are ~~number of~~ fragment features ~~which~~ have been used to guide the reconstructions process (25; 13; 21; 23; 15; 14; 41). The shape of the broken edge and the resulting fracture surface is likely to match and unlikely to intersect for neighbouring segments. When reconstructing hollow artifacts, the thickness of the fragments can be considered. The object surface can provide spatial information through the texture, superficial patterns or markings, and expected smoothness. The robustness of these features depends on the geometry and surface properties of the artifact, the number of missing fragments, and the quality of the preservation. Some reassembly algorithms are fully automated (21; 25**?**) while others rely on regular input from experts in the field, either for verification (15; 14) or to guide reconstruction (23; 41). Information ~~which guides experts~~ such as surface properties of the fossil ~~fragments providing~~ information regarding the mechanical properties of fossilizing bone under loading conditions. Fractures form in the presence of resistance against plastic deformation, where the peak forces are localized within the cracks and parts are dislocated rather than distorted. Conversely, less fragmentation and dislocation is generally indicative of plastic deformation. This information is used to guide expert users in computer-assisted manual reconstruction (23).

4.1 Fractured surfaces

The state of the art procedure for reassembling broken objects is a collection of algorithms which match fractured surfaces to successfully reconstruct the original form (13). The procedure assumes minimal ~~erotion,~~ such that fractured surfaces still contain sufficient similarity in terms of surface roughness and shape. It is also assumed that the original and ~~fracture faces are~~ sufficiently differentiable to allow for recognition using ~~the contrast~~ in roughness.

To classify surface types of the fragments, the user manually selects ~~point~~ from each set of surfaces. A supervised learning procedure builds a statistical model of the bend-

ing energy over the local neighbourhood which is used characterize classes of surface roughness.

Pairs of fractured surfaces ~~are~~ matched using clusters of patches with similar surface ~~roughness, with multiresolution~~ correspondences ~~used~~ more robust verification. Pair-wise correspondences are pruned based on the comparision of the cluster principal components and the geometric consistency of the matches. For all remaining pairs, the transformation required to fit the matching surfaces is computed. Using a graph based approach, cycles with compatible transformations are found to ensure global consistency of multi-piece matches. During this procedure, collision detection is employed to prevent penetration.

Given a confirmed match, constrained ~~simultatneous~~ registration is performed to set fractured pieces into their final alignment. This registration is formulated as a ~~quadractic~~ optimization problem with linear non-penetration ~~cosntraints.~~ Finally, registered fragments are merged into a single virtual fragment ~~are~~ the procedure is repeated to find further global matches.

Huang et al. (13) solve the solve the reassembly problem, as ~~it is~~ presented. However it is questionable whether ~~such~~ a procedure would be directly applicable to excavated artifacts or fossil ~~specimen.~~ Due to erosion and deformation, the fragmented surfaces alone might not provide sufficient information to reassemble the object. Also, often fragments of the fossil are not directly connected. Although the algorithm allows for missing data, it would not be able to position and orient single fragments without a model of the surface shape or an estimate of the profile curves as used by *The SHAPE Lab* in their reconstruction algorithm specialized for fragmented pots(**?**). In conjunction with manual guidance from an expert or by incorporating a more detailed model of surface shape, deformation and marking, the approach used in Huang et al. (13) has the potentially to greatly ~~fascilitate~~ reconstruction procedures.

4.2 Archeological applications

An ambitious archeological project ~~which~~ has been ongoing for centuries the reconstruction of the Severan Marble Pan of Rome (Forma Urbis Romae) which depicts the ground plan of every architectural feature of the ancient city down to the detail of internal staircases. Only ten percent of the map still survives and that which remains is fractured into over a thousand pieces.

Three-dimensional models of the marble map fragments were extracted using a high resolution ~~lazer~~ scanner and photographs. The inscribed map on the surface of the fragments ~~has been~~ the primary source of information ~~for~~ matching. Fragment thickness and marble veining directions are also useful indicators, as is the smoothness of the underlying surface. Moreover, clamp holes, straight slab edges, and wedge holes on select ~~fragements~~ provide position and orientation information given the constraints on the original map wall.

A natural approach would be to attempt reassembly by automatic feature extraction. Instead, the fragments were manually annotated: the boundary of each fragment was traced and the topographic features, including the wall features, were labelled. Using these labels, pairs of fragments are compared and scored based on the number of matching aligned features. Those with the highest scores are returned to the user for verification, after which they can be considered as a single piece and the algorithm is reiterated. Similar topographic features and wall features are searched for ~~in~~ with independently queries.

Multivariate clustering is also used to identify potential matches by grouping fragments based on thickness, marble veining direction, and underlying surface roughness.

Treating each type of feature independently and considering only pairs of matches seems limited, as does relying on expert verification at every iteration. Recent automated matching has been shown to be successful on seemingly difficult cases (13). Due to the erosion of the fragments, fractured surface-based matching was not considered. However, given the fragments shown the most recent algorithm for fractured surfaces (13) might be prove to be helpful. As mentioned ~~early~~, incorporating more surface data into the reconstruction algorithm of Huang et al. (13) could significantly contribute to the Forma Urbis Project (**?** 15). Since both research projects ~~from Standford~~, one would expect such work in the near future.

Archeological applications have inspired reassembly algorithms specialized for certain types of artifacts, such as label dependent algorithms (15; 14) or shaped specific algorithms (**?**). Other approaches have been developed for arbitrary objects (21), culminating with the work of Huang et al. (13), as discussed above, which incorporates many of the earlier techniques while using more robust verification producing the best results.

4.3 Paleoanthropology applications

In the reconstruction of skeletal fossils, anatomical features and bilateral symmetry are used to recontruct the specimen. Current reconstruction techniques in paleoanthropoloty are ~~a~~ted by computational tools, such as symmetrical projections to facilitate alignment, however they are predominantly manual relying heavily on the expertise of the user. Computational reconstructions aim to minimize systematic bias such as classification assumptions and establish an essentially self-referential reconstruction, maximixing to use of intrinsic information while only including essential extrinsic data (23).

Zollikofer et al. (41) used two recon~~s~~tion protocols to reconstruct a virtual model of the skull fossil, TM266. The fragments obtained with a CT scan, were repositioned and ~~re-orient~~ to restore morphological continuity along fractures, suture and other anatomical features within and between bones. Both reconstruction techniques predominantly manual and both assume a linear model for the correction of taphonic distortion.

In the first approach, symmetrical and parallel anatomical features shared by all mammal crania were used to position and orient each fragment, taking into consideration the constraints imposed by visible well preserved temporal lines. When reconstructing with visualization software, isolated parts are mirror-imaged and directly compared with opposite well-preserved parts. Superficial characteristics (in particular, wear of the dentition or sutures along the surface) are used for alignment. Well-preserved regions are used ~~as~~ primary anatomical compass to adjust other positions. Constraints are provided from nearby fragments and known anatomical features. Visualization of complex spatial relationships between fossil fragment can be facilitated with the use of stereo glasses and a stereo screen (23). To compensate for a lack of tactile information, physical verification can be done at different stages of the reconstruction process through stereolithographic models.

In the second approach, fragments were positioned and oriented relative to one another using stepwise reduction of degrees of freedom. Translational degrees of freedom were first reduced, establishing morphological continuity between fragments along matching fracture lines. Rotational degrees of freedom between adjacent fragments were reduced

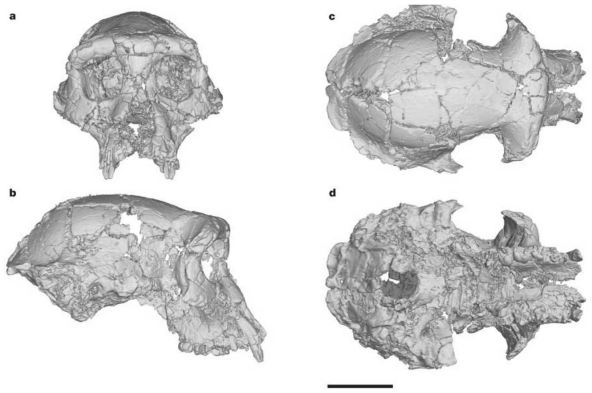

Figure 4: Average reconstruction of TM 266 cranium from Zollikofer et al. (41).

by step-wise inclusion of fragments into the reconstruction followed by iterative adjustments until a symmetrical integrated morphology was acheived. This approach was used to orient left and right sides relative to each other and the maxillae relative to midface. Almost complete preservation of TM266 largely facilitates this geometric reconstruction: contact between neighbouring fragments largely constrains the position and orientation of individual parts and bilateral symmetry ~~constraings~~ the overall morphology.

To verify the reliability of partial reconstructions, and ~~avoid~~ the ~~propogation~~ of local errors into the global reconstruction, anatomical subregions can be arranged independently instead of performing virtual reconstruction on the fossil as a whole (23). ~~As~~ an evaluation of the results, Zollikofer et al. (41) resonstructed the face and braincase independently and then assembled ~~by~~ using anatomical continuities. Common anatomical ~~contructs~~ can also be used to verify the validity of a reconstruction. Zollikofer et al. (41) ~~find~~ the posterior maximallary plane to be approximately perpendicular to the neutral horizontal axis of the orbits, as is the case in all mammals.

Despite a predominantly manual procedure, the variance between the reconstructions can be comparatively small. Zollikofer et al. (41) found the largest differences within 0.9mm, 1.1mm, and 2.3.mm -the average reconstruction is shown in Figure 4.

The virtual reconstruction of Zollikofer et al. (41) encountered several features which differ from earlier reconstructions: wider cranium, occipital contour is rounder sagitally, face is superiorly taller and relatively vertical, and a downward lipping of nuchal crest. In earlier work by Brunet et al. (8), estimated measurements are given from a preliminary three-dimensional reconstruction, however, the details of the reconstruction are not provided. The original sediment filled remains are shown in Figure 5.

4.3.1 Correcting Deformation

~~The~~ reconstruction should enable the identification of patterns of in-vivo, postmortem, and postrecovery modifications, and analyze their impact on fossil skeletal structures. In vivo, or epigenetic, alterations include natural modification such as asymmetry ~~incurring~~ through development or behavioural modification, pathologic modification from congenital malformations or traumatic injury, and artificial modification such as culturally moti-

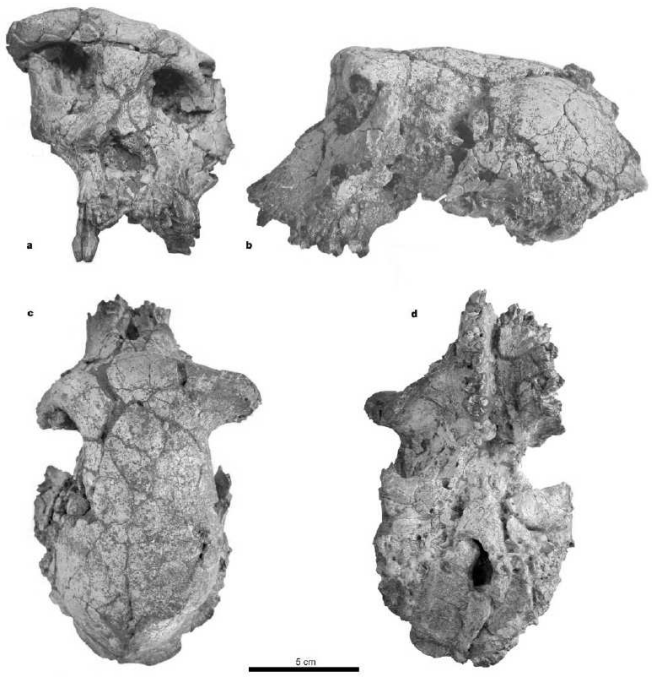

Figure 5: Original state of TM 266 cranium from Brunet et al. (8).

vated deformation. Postmortem alterations ~~include~~ biological modification resulting from predation, scavenging, ~~or~~ culturally motivated actions such as multiple burials, cremation, or cannibalism, diagenetic modification resulting from geo-physical processes, such as weathering, embedding, remineralization, taphonomic deformation, tectonic events, and process modifications resulting from removing the fossil from it original surrounding material, preservation by means of chemical treatments, and earlier reconstructions. Distinguishing between the biological and the geological causes for fossil distortion is often a source of debate ~~within the~~ paleontological research (37). Influences which cause deformation are ~~complex, difficult~~ to isolate and the process is complicated by the fact that the deformation order is reversed.

The full diagenesis process is extremely complex therefore rarely incorporated into fossil analysis. Observed compression of a fossil induced by the pressure of overlaying strata, either from gravitational force or lateral tetonic shift, will depend on the orientation of the fossil relative to the strata . Even considering only a simple underlying diagenetic model, the same ultimate fossil geometry can be brought about by various transformations starting from various original forms (23). In paleoanthropology, a simple linear deformation model is a commonly interpreted as the source of taphonic alterations and the remaining nonlinear deformation is attributed to in vivo alterations(23; 41).

Anatomical knowledge facilitates the verification of potential in vivo alterations. Ponce de León et al. (23) concluded that asymmetry found in *Le Moustier* was due to in vivo ~~trama~~ from hints of bone resorption on the surface, a lack of erosion within the area in question, and anatomical asymmetries exhibited in nearby regions which frequently ac-

company impact from injury in adolescent modern humans.

Supporting evidence for in vivo trauma could be identified using a more detailed model of the fossil and a simulation of impact. The shape and density of a bone is correlated to its potential for load bearing during the lifetime of the organism (22) and weight from stata post-mortem. Expert diagnostics are invaluable and far surpass what can currently be acheived with computers. Nonetheless, simulations using accurate bone models would contribute supporting physical evidence for their hypotheses regarding in vivo trauma and taphonimic distortion.

5 Statistical Analysis

Traditional morphometric analysis applied multivariate statistics to linear distances, ratios, counts, and angles. Unfortunately, these standard measurements provide only a limited description of shape. Size correction is required prior to comparision and the paleoanthropological community lacked ~~concensus~~ on a standard technique (1). Moreover, the accuracy of shape comparisons based on linear distances is somewhat questionable. Homologous correspondences could not be expected. For example, the maximum distance ~~is~~ cannot be defined by homologous landmarks since its location ~~is changes~~ between objects. Relative location of distance measures was not ~~measured, therefore,~~ identical measures could result from different shapes. The linear distance shape statistics do not preserve geometric relationships.

The fundamental shift in the methodology for comparative analysis of biological shape and deformation has been called the geometric morphometric revolution (1). The change was motivated by ideas introduced by D'Arcy Thompson in 1917(32). However, these concepts were not formulated mathematically until Bookstein et al. (**?**) and the use of these morphometric tools did not prevail until ~~code~~ was ~~provide~~ to the anthropological community by (**?**).

~~Under this 'new' paradigm,~~ rather than measuring sets of distances between homologous features, configurations of features ~~are~~ considered and analyzed statistically as an ensemble (40). Analyzing the geometric information about the relative feature positions provides a more comprehensive and comparable analysis of shape.

5.1 Features

5.1.1 Landmarks

Landmarks are selected to provide correspondences and thereby faciliate comparison. Based on knowledge of ~~comparitive~~ anatomy and developmental biology, the locations chosen are considered developmentally homogeneous. Locations are typically selected such that they are homologous across ~~specimen,~~ based on anatomical structures that perform the same function for different biological species which evolved from a common ~~ancestor~~ species (7). Moreover, for an informative shape analysis landmarks should be optimal descriptors. This introduces issues with respect to handling missing data when performing statistical shape analysis, since optimal shape descriptors are not necessarily homologous.

Landmark placement and correspondence assignment can be time consuming, even with the assistance of specialized software. As a result the number of landmarks is often

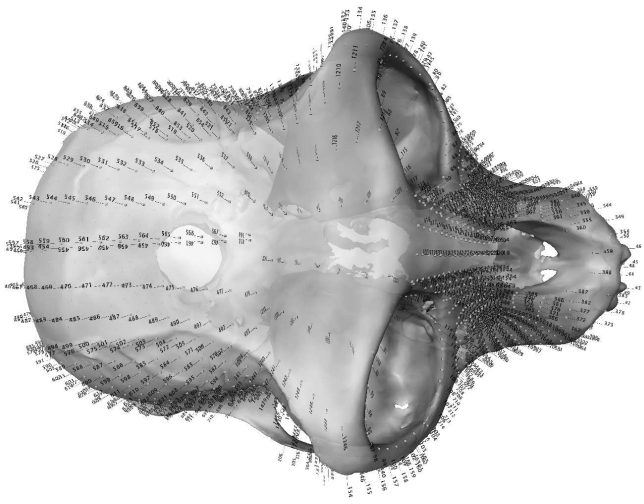

Figure 6: A full set of 853 landmarks placed on the scanned ~~crania~~ of an Old World Monkey. These were landmarks, created in the ~~speciliazed~~ software, used 45 are single points, 32 curves and 9 surface patches. (38)

~~to few~~ to capture an accurate shape description (38).

Sliding landmarks were introduced by Bookstein et al. (**?**) to better capture the shape changes between the landmark locations. Following least squares alignment of the homologous landmarks, a collection of semi-landmarks are placed along the object outline or surface to capture the shape between pre-existing landmarks. These semi-landmarks are fixed in position on the reference object and shifted along the outline or surface of each specimen, in an order preserving manner, until they are optimally fit to the corresponding reference points with respect to the tangential least squares error. The use of semi-landmarks provides a much richer description of shape (see (38) relative to (23)). Given sufficiently similar shapes, such as the skulls from various species of monkeys, the sliding step is not ~~required using~~ evenly spaced semi-landmarks suffices (38).

5.1.2 Salient Lines

Using continuous lines directly captures the shape of the surface, instead of using discrete landmark-based methods which require splines to subsequently approximate the shape. Salient lines along the object surface have been explored as shape descriptors for skeletal fossils (31**?**), similar to wires deformers (29). These lines, known as crest lines (31), creases or ridge lines (**?**), are defined by the extrema of principal curvature with the largest absolute magnitude. Salient lines have been described manually allowing the user to choose features which incorporate anatomical knowledge, describe the morphology, and correspond to homologous regions(4). Automatic extraction of crest lines captured many of the anatomical ridges incorporated in the manual approach. Unfortunately, the results also included a significant amount of spurious data, as illustrated in Figure 7. Also, independent extraction of features on each skull no longer guarantees correspondence aresulting in a complicated matching process. Nonetheless, the results of matching crest

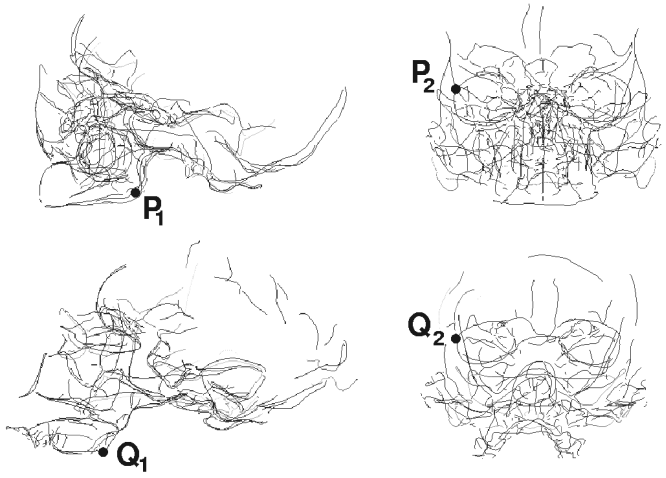

Figure 7: Crest lines automatically extracted from two skeletal specimen: Modern Man (536 lines and 5756 points) shown above and Man of Tautavel (337 lines and 5417 points) shown below. Crest line do extract salient features, however they also attract a signifcant number of other suprious features. Correspondences between these crest lines are difficult to determine, for example, the pairings (P1, Q1) or (P2, Q2).

lines and morphing the shape between the skull is visually impressive (17).

5.2 Alignment

The use of landmarks prevails throughout the paleoanthropological literature and as a result, statistical methods are predominantly landmark-based. Landmark homology is assumed to be known.

5.2.1 Procrustes Superimposition

In physical anthropology, pairs of specimen are commonly aligned using procrustes superimposition. Using this aligment procedure, one shape is chosen as the reference shape. The other shape is translated to the common origin, then scaled and rotated to minimize summed squared interlandmark distances (called the procrustes distances). Unfortunately, minimizing pairwise procrustes distances does not produce an optimal multiple alignment. To obtain a multiple alignment, a concensus or reference shape is determined onto which all specimen superimposed -a procedure called General Procrustes Alignment (GPA). Shape variation is commonly analyzed through the Procrustes coordinates, the landmark coordinates transformed into the common geometric space.

5.2.2 Repeated mean fitting

When two shapes are superimposed within an appropriate context, the similarities and differences become apparent. When change has taken place primarily in a localized region, by perfectly superimposing the unchanged region the changed region can be easily

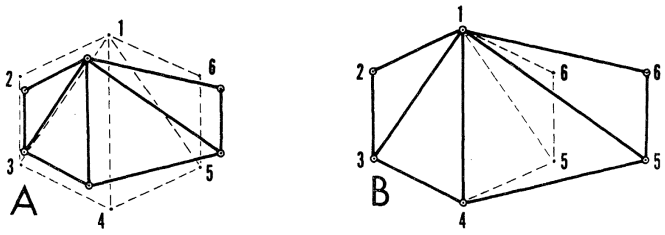

Figure 8: The results of two shape transformation techniques given homologous point correspondences. Least squares fit of the shapes is shown in *A* and the repeated mean fit of Siegel and Benson (27) is shown in *B*.

identified by its lack of fit and large residuals. The least squares solution finds the transformation which minimizes the sum of squared differences over all landmark points; regions with large deformations will have a large impact on the fit, therefore the true shape differences are obscured. A resistant technique, such as the repeated mean technique (27) limits the influence of large deformations in such a way that the resulting fit remains close in similar regions and not close in relatively deformed regions.

In the repeated mean fitting of Siegel and Benson (27), scale and rotation parameters are estimated separately. The correspondence between homologous points is assumed to be known and any necessary reflection has been performed. For any two points, consider the ray which connects them. The scale and rotation factors adjust the ray in one shape to correspond to the homologous ray in the second: the scale factor transforms the length of the ray, and the rotation factor transforms the direction or angle of the ray. The doubly-repeated median is used to determine the correct factors: given n homologous points, take the median of the n medians of the $n-1$ scale factors associated with segments from each point and similarily with the rotation factor.

Assuming deformation has taken place predominantly in a localized region, we can interpret the deformed points as outliers. The breakdown point of an estimator is smallest fraction of outliers that can cause the estimator to deviate arbitrarily from the estimate performed on the uncontaminated sample. For least squares, any outlier will alter the correct solution whereas for the repeated mean approach over half the samples must be outliers before the solution is corrupted. The example in Figure 8 illustrates the benefit of using the repeated mean criteria to emphasize localized deformation. When applied to archeological applications such as the skulls in Figure 9, the correct fit is less obvious to a non-specialist (especially when the scaling factors are variable). The vector representation in Figure 9 shows the focus of variation on fewer positions in the repeated mean approach rather than averaged over all points as in least squares. Most clearly illustrated through these examples is the significant impact of the fitting criteria on the resulting interpretation of variation observed. Prior to selecting an approach, the assumptions inherent in the fitting criteria should be made understood and clearly stated.

These underlying ideas for aligning and comparing homologous sets of landmark-coordinates were introduced by Thompson (32) and a mathematical description was formalized by Bookstein (**?**). Despite this early introduction of the concepts within archeological literature, the techniques were not widely applied until Siegel and Benson (27) published the algorithm which scientists could implement and apply to their existing land-

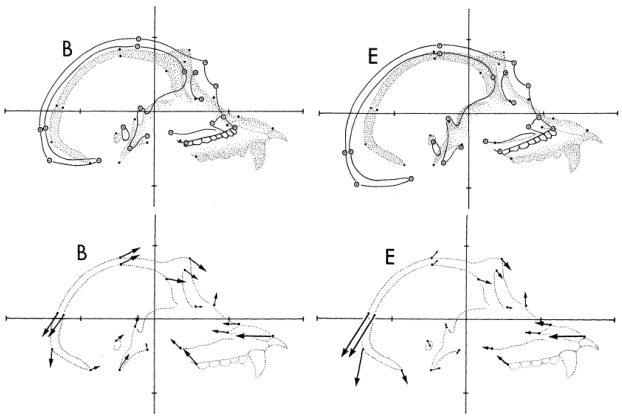

Figure 9: The fitting of a human skull of Australopithecus (A, D), Homo erectus (B, E) and Homo sapiens (C, F) to a chimpanzee skull (shown shaded). Least squares ($A - C$) and the repeated mean fit ($D - F$) of Siegel and Benson (27). The upper image shows the superimposition of the two skulls and the bottom shows the chimpanzee skull with vectors indicating the change in position of homologous points.

mark data.

Although the algorithm itself is not widely used, the principals behind the approach are found within the literature, applied in a supervised manner to the analysis of cranial profiles (5). Traditional anatomical landmarks were projected onto the midsagittal plane and semi-landmarks were placed along each external and internal curve of the frontal skull. The inner profile of the skulls were virtually indistinguishable after the procrustes superimposition, however the outer profile still exhibit significant variation. Instead of optimizing the overall fit, the shape of the outer profile was analyzed, given inner profile fit.

5.3 Comparative Morphometric Analysis

Allometry, a linear approximation of the dependence of shape on size, is often used in physical anthropology for the statistical analysis of the relationship between skeletal remains. Allometry for interlandmark distance data is often estimated with multivariate regression of the principal components of the procrustes coordinates on the log of the specimen size, determined by the scaling factor. Overall allometry can be considered consistent between species only if all bivariate allometries are the same for the two species. Multivariate methods should be used to test global allometric scaling (18).

Relative warp analysis is the most widely used approach in the study of shape variation (12; 9; 23; 41). Relative warp analysis is the analysis of the principal components of the Procrustes shape coordinates. The principal components are determined using the eigendecomposition of the covariance of the data. Analysis is performed on the subset of the principal directions which account for the highest-variation in the data.

Singular warp analysis, known as partial least squares analysis in the statistical literature, is an alternative approach to shape analysis used by Bookstein et al. (6) to capture independent sources of variation in the craniofacial complex of skeletal remains reveal-

ing independent shape variation between the phylogenetic and ontogenetic processes. In comparison, relative warp analysis refers to prediction of the shape variation as a whole, whereas singular warp analysis refers to predictions of shape variation in seperate regions where the relationship between directions of variation in the regions is as strong as possible.

Within this context it is important to reiterate the principal components are statistical constructions forced to be mutually uncorrelated. When analyzing data spanning several anatomical regions over several specimens, these components do not correspond to actual biological factors, which are rarely be completely independent.

Despite the availability of three-dimensional data, analysis is generally performed in the two-dimensional plane (5; 9; 12; 36). This issue has been attributed to a variety of causes (1). Although two-dimensional morphological variation is easier to visualize, it is inherently limited.

5.4 Specific Applications

5.4.1 Endocranium

Falk et al. (9) use three-dimensional CT reconstructions of the internal braincase of specimen *LB1*, for comparative analysis with a broad selection of samples including chimpanzees, Homo erectus, contemporary humans, gorillas, among others. A table presented standard linear distance measures (length, height, breadth, frontal breadth) and ratios between these, obtained from the endocasts. Measurements were taken from the basal view of the endocasts and projected onto the horizontal plane and the first three principal components of these are compared for each sample. Through these and other visualization methods the authors discuss the relative shape properties of the specimen and potential phylogenetic relationships between LB1 and other specimen. Although there conclusions are very extensive, the mathematical morphometric evidence is limited.

5.4.2 Wrist bone analysis

Following the excavation procedures and fossil reconstruction paleoanthropolgists move to the statistical analysis of the data obtained. This analysis involves describing the anatomy and comparing it to other fossils of similar antiquity, determining shared species characteristics, the chronological age of the specimen, the sex, and any unique features of the individual. Using the information inferred from the excavated remains, paleoanthropologists aim to place the organism into broader phylogenetic and, when appropriate, ontogenetic context.

The bones of the wrist have played a significant in establishing, in some sense indirectly, the phylogenetic context for discovered hominid specimen. Biomechanical and funtional capabilities have been explored looking at the external properties, notably the surface morphology (34), and the internal properties, notably bone density (22).

In (34), an analysis of the morphology of the trapezium in both extant and extinct species lead to hypotheses on the functional capabilities of the latter. The articular surfaces of the trapezium were describe by two-dimensional planes, optimally fit in the least squares sense. The relative angles between these planes form distint categories, shown in Figure 10. For the extant species, they present a mapping from these categories to functional abilities, that seperates species with the superior object manipulation capabilities,

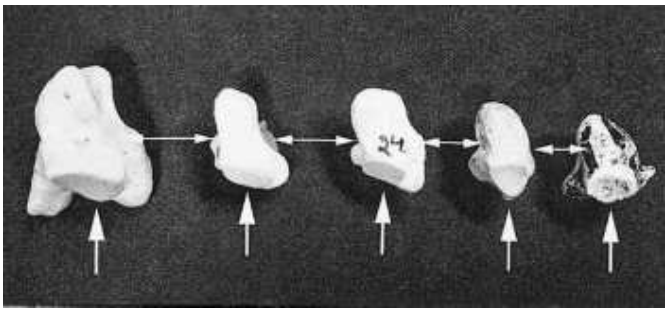

Figure 10: Articular surfaces on the trapezium showing the relationship between the trapezoid (horizontal arrows) and scaphoid (vertical arrows). Shown from left to right: gorilla, chimpanzee, human, A.L.333-80, and O.H.7-NNQ.(34)

such as grasping, from those who use their hands for more basic manipulation and locomotion. By classifying the fossil morphology of extinct species, functional capabilities are inferred.

In (22), the apparent bone density patterns of the distal radius were compared across several primate groups which are known to have diverse hand postures for quadrupedal location: apes which are knuckle-walking, monkeys which walk with pressure on their digits, and monkeys which walk with pressure flat on the palms. Bone density measures in the subchondral cortical plate of bone of the distal radius can be used to evaluate the mechanical load experienced by the wrist joint in different hand postures, as shown in Figure 11. Classifying these bones by loading pattern results in a grouping of primates that similar habitual hand postures adopted during quadrupedal locomotion, as shown in Figure 12 This information can be extrapolated to infer the hand postion adopted by extinct species.

6 Modeling

In the context of paleoanthropology, modeling attempts to capture in vivo characteristics of the extinct species from information inferred using excavated fossils and extrapolated using relationships with extant species for which more data is available.

6.1 Biomechanical Modeling

The lack of a physical record of the musculature of a given fossil specimen means biomechanical studies are limited. Nonetheless, morphological similarities between a fossil and the human skeleton provide a basis for extrapolating available human data. The skeleton of *Australopithecus afarensis*, known as "'Lucy"', is the most complete source of locomotor morphology currently available for early hominids. There is conflicting evidence in the literature regarding the form of Lucy's bipedal locomotion. Some hypothesize her manner was similar to chimpanzee locomotion with the hips and knees bent, while others claim her manner ressembled upright humans motion where the legs are kept relatively straight.

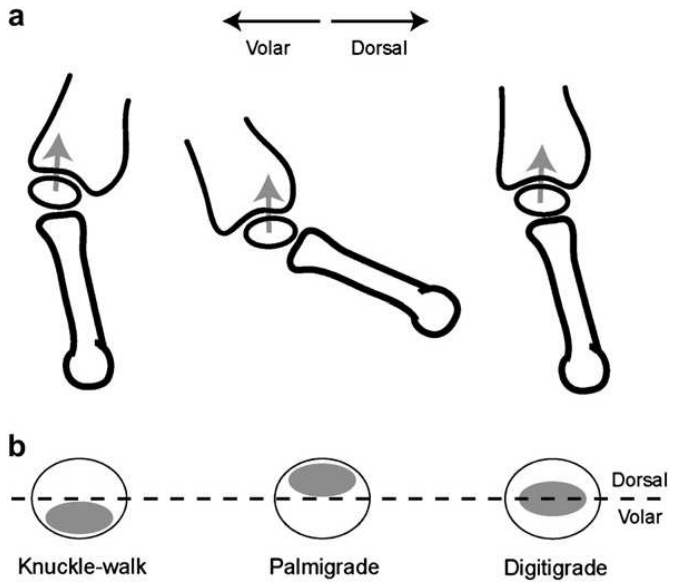

Figure 11: (a) Drawing of the wrist joint depicting the hand postures of different quadrupedal locomotive styles shown at mid-support of stance phase, shown from left to right: knuckle-walking, palmigrade, digitigrade. The hypothesized orientation of compressive forces are shown by gray arrows. (b) Schematic illustration of the distal radial articular surface, with the gray ovals predicting areas of high apparent density.(22)

Nagano and Umberger (19) map human musculature data onto Lucy's skeleton and perform similations to evaluate whether or not Lucy could have walked in an upright, straight-legged manner with an energetic cost similar to that of modern humans.

The simulations by Nagano05 and Umberger (19), muscle origins, insertions and via-points were located by combining Lucy's geometry with human anatomy. A Hill muscle model was used with the parameters, physiological cross-sectional area (PCSA) and maximum isometric contractile element force values, derived by scaling human muscle data. The relative body segment inertial parameters were also based on relations reported for humans.

Skeletal movement is motivated by muscle activation, which is specified in their model by the onset and offset time and the activation value. Using the approach developed by Anderson and Pandy (3), the activation parameters are determined over a single step and the results were relfected for the second. The activation parameters are learned by minimizing the difference between the simulated posture at the end of the first step and a typical upright human-like target posture, the difference in angular velocity between beginning and end of the step, and the whole body energy expenditure per meter. Energy expenditure is measured as mechanical work (muscle power integrated over time) and heat (sum of activation heat, maintenance heat, and shortening/lengthening heat). Ground/foot interaction was done as Anderson and Pandy (3)

Despite the reliance on human data, Nagano and Umberger (19) claim the model of Lucy presents more than a scaled down human. Morphological features of Lucy's skeleton

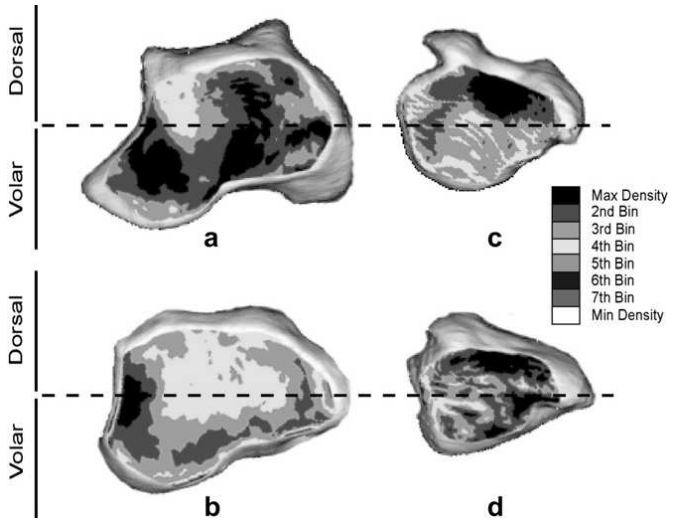

Figure 12: Apparent bone density maps of the distal radial articular surface superimposed on three-dimensional reconstructions of the bone. The surfaces are separated into dorsal and volar regions by a dashed line. The density patterns correspond to hand posture, with high density regions in black: gorilla uses knuckle hand postures for locomotion (a); the hominid, Pongo pygmaeus, varies between hand postures when walking quadrupedally (b); Papio ursinus locomotes with a digitigrade hand posture (c); and Nasalis larvatus locomotes using palmigrade hand postures (d).(22)

differ from those of modern humans, which effects the musculature. In particular, the wider pelvis provides the lower limb muscles with a larger moment generating capacity in the caronal/transverse plane. Early biomechanical studies of locomotion have shown that rotation of pelvis in transverse plane is an important determinant in gait (26).

There were subtle differences, however gross joint kinematic patterns were found to be similar to data from human. The flexion/extention of the hip, knee and ankle was found to be similar to humans. However, the external/internal rotation of the hip was 50deg rather than the expected 20deg, due to the wider pelvis.

The simulation produced relatively smooth kinematics. Root mean squared difference in angle between the initial and final posture was greater than maximal intra-subject deviation found in gait studies for humans. The source of the difference was concentrated in ankle inversion and metatarsal joint angle. Since foot morphology was not available for Lucy, scaled data from another hominid specimen was used as an approximation. It is claimed that the error could be reduced with more iterations of the optimization procedure, however this was not illustrated and would need to be to support the claim that compuational power is the sole obstacle.

Nagano and Umberger (19) found the muscle activation profiles to be qualitatively similar to EMG recording during modern human locomotion. Most muscles had comparable muscle activation parameters, however for some muscles the activation was greated. [2] The wider pelvis requires a larger hip abduction moment to keep trunk upright during

[2] Without prior experience in analysis of EMG plots it is difficult to assess the extent of similarity.

stance phase.

The average walking speed was slower than expected given Lucy's body height.

Although energy expenditure in the simulation was higher than modern human adults, it was similar that of children with the same body mass as Lucy. The mechanics of chimpanzee walking with bent hips and knees, although a source of greater postural stability, it requires more energy to maintain the posture. It would have been possible to adjust the initial and final postures to a stance similar to that of the chimpanzee and explore energy expenditure, however this was not included.

This simulation confirms that if Lucy had a musculature similar to a human, it could have been possible that she walked in an upright straight-legged manner. This work does not provide strong evidence supporting human-like bipedal locomotion, rather it doesn't contradict that hypothesis.

Further analysis with respect to the difference between chimpanzee and human locomotive musculature, and the impact of this difference on energy expenditure would be helpful to assess the results presented. As would more information regarding the effect of a wider pelvis on the gait perhaps in other species, if it is available. An animation of the results is not provided.

6.2 Facial Modeling

Automatic facial reconstruction has been applied to predict the appearance of members of extinct civilizations. Described as an application for crest line morphometry (31), the deformation between a human skull and the fossilized skull is calculated. This deformation is then applied to the face of the human skull to infer the unknown face. The results are difficult to assess from the given images, shown in Figure 13. One would suspect that the results could be improved using techniques developed in computer graphics on facial animation. Perhaps by using a more detailed anatomical model such as a finite element model incorporating muscle data (28) and extrapolating from human musculature as in biomechanical models (19).

7 Visualization

Early work in three-dimensional statistical shape analysis and modeling, using 31 landmarks for a wire frame model (20), provided minimal information for reconstruction. The graphical illustrations are simple, demonstrating the information used in the statistical analysis, however they are drastically inadequate for visualization. With the influence of computer scientists, graphical representations of morphology quickly progressed.

Bookstein et al. (6) also used extreme simplified graphical representations to reason about patterns in ontogeny and phylogeny, shown in Figure 15. Given the graphical techniques available analysis using side-by-side comparison of the rough grids can be significantly improved. The visualization of morphometrics is significantly superior in the earlier work of (31), as shown in Figure **??** and illustrated in the video (17).

Although most analysis is now done using three-dimensional models, the shape comparisons are often described in words rather than images. Falk et al. (9) use a three-dimensional CT reconstructions to analyze the internal braincase of specimen *LB1*. Using virtual models of the endocasts scaled to a common size, the authors dicussed general shape differences through a basic visual comparison. Using anatomical knowledge the

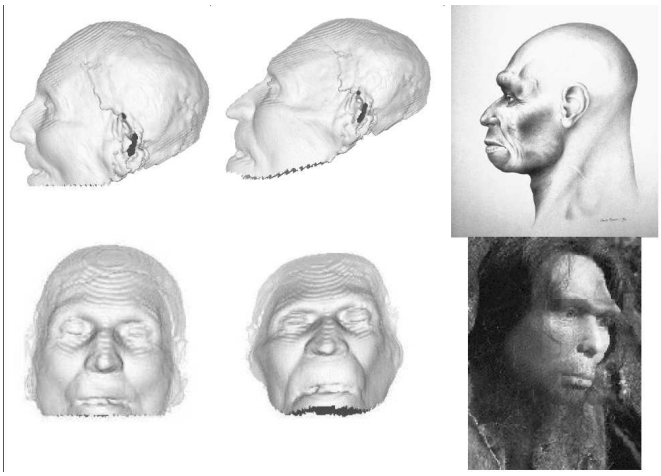

Figure 13: Automatic facial reconstructions are compared with illustrated interpretations. The reference human is shown on the left, the inferred Man of Tautavel is shown in the centre. (31)

expected contours, vessels, veins, notches and depressions are located shown as seperate sketched as a medical illustration. Through these methods, and statistical approaches discussed earlier, the authors discuss the relative shape properties of the specimen and potential phylogenetic relationships between LB1 and other specimen.

7.1 Phylogenetic Trees

A recent interdisciplinary publication by Wiley et al. (38) was evidently influenced by the computer science community and is the most elegant of research paper included in this review. The morphometric principals are described in a straightforward manner and the assumptions and limitations stated clearly. In their work, the phylogenetic/evolutionary tree of monkey species is illustrated visually, as shown in Figure 16. Given an evolutionary tree based on genomic data, the three-dimensional virtual models of the existing species are weighted and linearly interpolated to create hypothetical crania of extinct ancestors. The statistical morphometric techniques used, such as thin plate spine interpolation and general procusts alignment, are common throughout the paleoanthropological and geometric morphometry literature. The merging of the noisy mesh data is handled using an extremal surface contruction, drawn from computer science literature. Evolutionary trees have been developed using morphological distance measures (16), however, in this work the trees are based on molecular data and the morphometry is weighted based on these genomic distance measures.

8 Conclusion

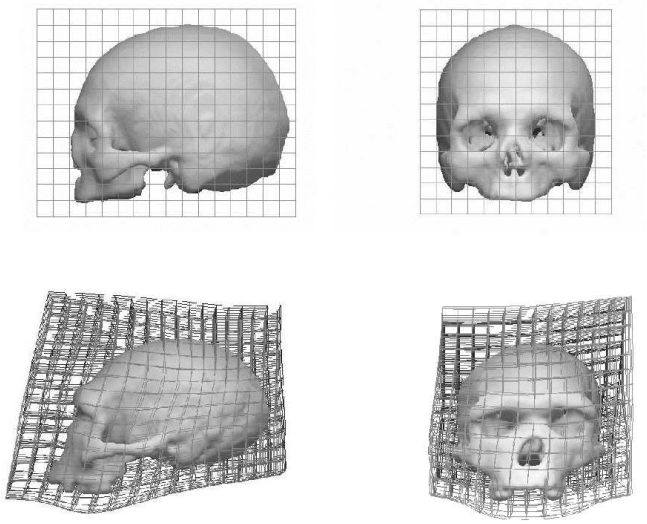

Figure 14: Deformation of the Man of Tautavel skull, shown below, and the reference human skull shown above. (31)

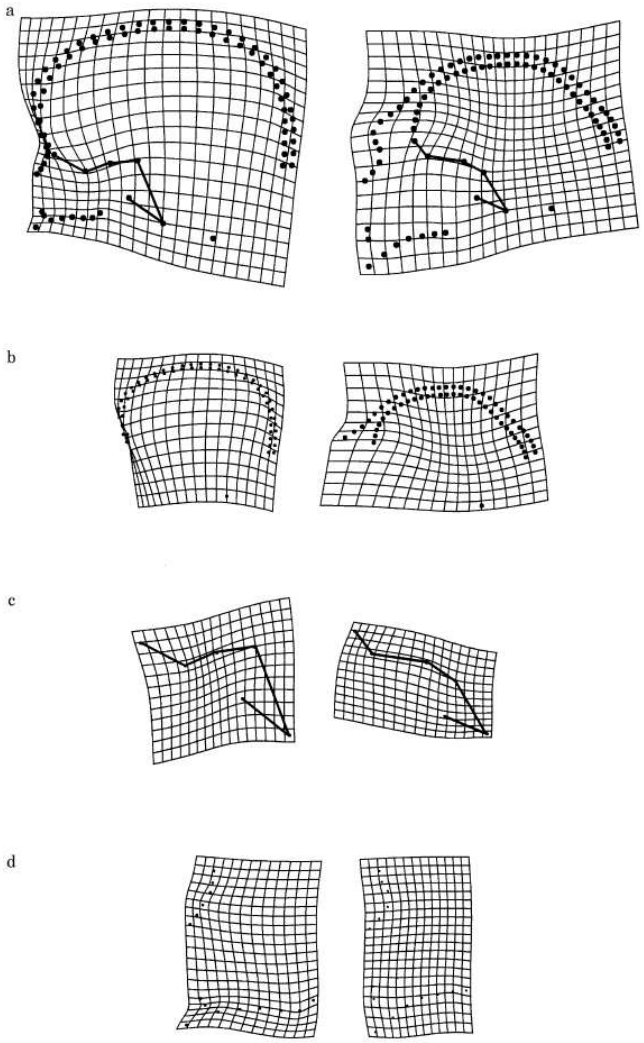

Figure 15: First singular warp for the subset adult Homo specimens: *(a)* shown as a composite spline and for each of the three components separately: *(b)* vault *(c)* cranial base and *(d)* face. Left and right pairs illustrate the directions of deformation for the block involved, of arbitrary magnitude. The deformations is each column are positively correlated. Using these graphical representations, Bookstein et al. (6) descsribe the deformation in the left column as moving toward the modern specimens exhibiting comparatively smaller face, relatively larger neurocranium, and thinner vault, and the deformation toward the right column as archaic at the robust extreme of the forms with relatively larger faces and thicker vault bones.

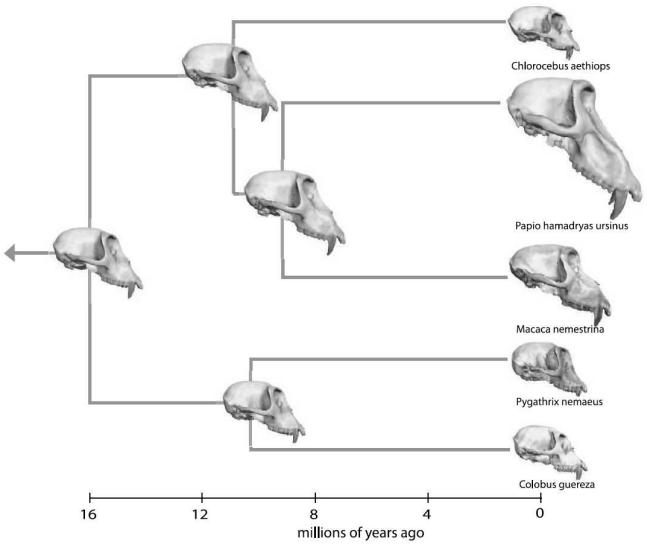

Figure 16: The input surface meshes, shown on the leaves of the tree, were obtained from laser range scans of the crania of existing monkey species. The surface meshes at the internal nodes represent the skull shapes of the hypothetical ancestors, as computed using our system. The length of the branches of the tree correspond to the estimated dates at which the species are hypothesized to have diverged. (38)

References

[1] Dean C. Adams, F. James Rohlf, and Dennis E. Slice. Geometric morphometrics:ten years of progress folloing the 'revolution'. *Italian Journal of Zoology*, 71:5–16, 2004.

[2] K. Ahluwalia. *Knee joint load as determined by tibial subchondral bone density: its relationship to gross morphology and locomotor behavior in catarrhines*. PhD thesis, State University of New York at Stony Brook, 2000.

[3] Frank C. Anderson and G. Pandy, Marcus. Dynamic optimization of human walking. *Journal of Biomechanical Engineering*, 123:381–390, October 2001.

[4] F. L. Bookstein and C. B. Cutting. A proposal for the apprehension of curving cranofacial form in three dimensions. In *Cranofacial Morphogenesis and Dysmorphogenesis*, pages 127–140, 1988.

[5] Fred Bookstein, Katrin Schafer, Hermann Processinger, Horst Seidler, Martin Fieder, Chris Stringer, Gerhard W. Weber, Juan-Luis Arsuaga, Dennis E. Slice, F. James Rohlf, Wolfgang Recheis, Ato J. Mariam, and Leslie Marcus. Comparing frontal cranial profiles in archaic and modern *homo* by morphometric analysis. *The Anatomical Record*, 257:217–224, 1999.

[6] Fred L. Bookstein, Philipp Gunza, Philipp Mitteroecker, Hermann Prossinger, Katrin Schfer, and Horst Seidler. Cranial integration in homo: singular warps analysis of the midsagittal plane in ontogeny and evolution. *Journal of Human Evolution*, 44(2):167–187, 2003.

[7] Ingo Brigandt. Homology in comparative, molecular, and evolutionary developmental biology: The radiation of a concept. *Journal of Experimental Zoology Part B: Molecular and Developmental Evolution*, 299B(1):9–17, 2003.

[8] Michel Brunet. A new hominid from the upper miocene of chad, central africa.

[9] Dean Falk, Charles Hildebolt, Kirk Smith, M. J. Morwood, Thomas Sutikna, Peter Brown, Jatmiko, E. Wayhu Saptomo, Barry Brunsden, and Fred Prior. The brain of lb1 *homo floresiencsis*. *Science*, 308:242–245, April 2005.

[10] William L. Fink. The conceptual relationship between ontogeny and phylogeny. *Paleobiology*, 8(3):254–264, 1982.

[11] Janet C. Gardner, Greg Garvin, Andrew J. Nelson, Gian Vascotto, and Gerald Conlogue. Paleoradiology in mummy studies: the sulman mummy project. *Canadian Association of Radiologists Journal*, 5(4):61–76, October 2004.

[12] Franck Guy, Daniel E. Lieberman, Daniel E. Pilbeam, Marcia Ponce de Leon, Andossa Likius, Hassane T. Mackaye, Patrick Vignaud, Christoph Zollikofer, and Michel Brunet. Morphological affinities of the *sahelanthropus tchadensis* (late miocene hominid from chad) cranium. *PNAS*, 102(52):18836–18841, December 2005.

[13] Qi-Xing Huang, Simon Flory, Natasha Gelfand, Michael Hofer, and Helmut Pottmann. Reassembling fractured objects by geometric matching. *ACM Transactions on Graphics, SIGGRAPH*, 25(3):569–578, 2006.

[14] David Koller and Marc Levoy. Computer-aided reconstruction and new matches in the forma urbis romae. *Bullettino Della Commissione Archeologica Comunale di Roma*, 2005.

[15] David Koller, Jennifer Trimble, Tina Najbjerg, Natasha Gelfand, and Marc Levoy. Fragments of the city: Stanford's digital forma urbis romae project. *Journal of Roman Archaeology supplement*.

[16] Charles A. Lockwood, William H. Kimbel, and John M. Lynch. Morphometrics and hominid phylogeny: Support for a chimpanzee-human clade and differentiation among great ape subspecies. *PNAS*, 101(13):4356–4360, March 2004.

[17] Bertrand Mafart, Denis Mline, Alain Silvestre, and Grard Subsol. Imagerie 3d et palontologie : les diffrences de forme entre le crne de l'homme moderne et de l'homme de tautavel (v.1), 1999.

[18] Philipp Mitteroecker, Philipp Gunza, and Fred L. Bookstein. Heterochrony and geometric morphometrics: a comparison of cranial growth in pan paniscus versus pan troglodytes. *Evolution & Development*, 7(3):244–258, 2005.

[19] Akinori Nagano, Brian R. Umberger, Mary W. Marzke, and Karin G. M. Gerritsen. Neuromusculoskeletal computer modeling and simulation of upright, straight-legged, bipedal locomotion of *australopithecus afarensis*. *American Journal of Physical Anthropology*, 126:2–13, 2005.

[20] Paul O'Higgins and Nicholas Jones. Facial growth in *cercocebus torquatus*: an application of three-dimensional geometric morphometric techniques to the study of morphological variation. *Journal of Anatomy*, 193:251–272, 1998.

[21] Georgios Papaioannou and Evaggelia-Aggeliki Karabassi. On the automatic assemblage of arbitrary broken solid artefacts. *Image and Vision Computing*.

[22] Biren A. Patel and Kristian J. Carlson. Bone density spatial patterns in the distal radius reflect habitual hand postures adopted by quadrupedal primates. *Journal of Human Evolution*, 52:130–141, 2007.

[23] Marcia Ponce de Leon and Christoph P. E. Zollikofer. New evidence from le moustier 1: Computer-assisted reconstruction and morphometry of the skull. *The Anatomical Record*, 254:474–489, 1999.

[24] Marcia S. Ponce De Leon. Computerized paleoanthropology and neanderthals: The case of le moustier 1. *Evolutionary Anthropology: Issues, News, and Reviews*, 11(S1):68–72.

[25] The SHAPE Lab STITCH project. Assembling virtual pots from 3d measurements of their fragments.

[26] J.B.D. Saunders, V.T. Inman, and H.D. Eberhart. The major determinants in normal and pathological gait. *Journal of Bone Joint Surgery [Am]*, 35:543–558, 1953.

[27] Andrew F. Siegel and Richard H. Benson. A robust comparison of biological shapes. *Biometrics*, 38(2):341–350, June 1982.

[28] Eftychios Sifakis, Andrew Selle, Avram Robinson-Mosher, and Ronald Fedkiw. Simulating speech with a physics-based facial muscle model. In *Eurographics/ACM SIGGRAPH Symposium on Computer Animation*, 2006.

[29] Karan Singh and Eugene Fiume. Wires: a geometric deformation technique. In *SIGGRAPH '98: Proceedings of the 25th annual conference on Computer graphics and interactive techniques*, pages 405–414, New York, NY, USA, 1998. ACM Press.

[30] Fred Spoor, Nathan Jeffery, and Frans Zonneveld. Using diagnostic radiology in human evolutionary studies. *Journal of Anatomy*, 197:61–76, 2000.

[31] G. Subsol, B. Mafart, A. Silvestre, and M.A. de Lumley. 3d image processing for the study of the evolution of the shape of the human skull: Presentation of the tools and preliminary results. In *XIV International Congress of Prehistoric and Protohistoric Science*, September 2001.

[32] D'Arcy Thompson. *On Growth and Form*. 1997.

[33] Jennifer L. Thompson, Andrew J. Nelson, and Bernhard Illerhaus. 3-d imaging and traditional mporphometric analysis of the adolescent neandertal from le moustier. In *Three-Dimensional Imaging in Paleoanthropology and Prehistoric Archaeology*, pages 55–61, Universite de Liege, Belgium, September 2002.

[34] M.W. Tocheri and ... Marzke, M. W. Functional capabilities of modern fossil homined hans: Three-dimensional analysis of trapezia. *American Journal of Physical Antrhopology*, 122:101–112, 2003.

[35] Jihong Wang and Timothy J. Blackburn. X-ray image intensifiers for fluoroscopy. *Radiographics*, 20:1471–1477, 2000.

[36] Gerhard W. Weber, Johann Kim, Arnold Neumaier, Cassian C. Magori, Charles B. Saanane, Wolfgan Rcheis, and Horst Seidler. Thickness mapping of the occipital bone on ct-data – a new approach applied on oh 9. *ACTA Anthropologica Sinica*, 19, Supplement:37–46, 2000.

[37] T.D. White. Early hominids–diversity or distortion? *Science*, 299:1994–1996, 2003.

[38] David F. Wiley, Nina Amenta, Dan A. Alcantara, Deboshmita Ghosh, Yong J. Kil, Eric Delson, Will Harcourt-Smith, F. James Rohlf, Katherine St. John, and Bernd Hamann. Evolutionary morphing. In *Proceedings of IEEE Visualization 2005*, 2005.

[39] J. Zapata, C. Prez-Sirvent, M. J. Martnez-Snchez, and P. Tovar. Diagenesis, not biogenesis: Two late roman skeletal examples. *Science of Total Environment*, 369(1):357–368, October 2006.

[40] Christoph P. E. Zollikofer. A computational approach to paleoanthropology. *Evolutionary Anthropology*, Supplement 1:64–67, 2002.

[41] Christoph P. E. Zollikofer, Marcia S. Ponce de Leon, Daniel E. Lieberman, Frank Guy, David Pilbeam, Andossa Likius, Hassane T. Mackaye, Patrick Vignaud, and Michel Brunet. Virtual cranial reconstruction of *sahelanthropus tchadensis*. *Nature*, 434:755–759, April 2005.